Combined Theoretical and Vibrational Study of Dihexylbithienoquinonoid Derivatives with Regioregular Head-to-Head, Head-to-Tail, and Tail-to-Tail Orientations

V. Hernández,[†] S. Calvo Losada,[†] J. Casado,[†] H. Higuchi,[‡] and J. T. López Navarrete*[,†]

Departamento de Química Física, Facultad de Ciencias, Universidad de Málaga, 29071 Málaga, Spain, and Department of Chemistry, Faculty of Science, Toyama University, 3190 Gofuku, Toyama 930-8555, Japan

Received: October 27, 1999

We present the results of a theoretical and vibrational spectroscopic study carried out on three different 2,2′-(dihexyl-2,2′,5,5′-tetrahydro-2,2′-bithienylidene-5,5′-diylidene)bis(propanedinitrile) isomers, which are compared with the corresponding unsubstituted bithienoquinonoid in the pristine state as solids. In these isomers, the two solubilizing hexyl side chains are attached to preassigned β-positions: head-to-head (HH), head-to-tail (HT), and tail-to-tail (TT). These materials possess a highly extended π-electron conjugation, since they bear a pure heteroquinonoid structure in their electronic ground states. Thus, these molecules could be regarded as suitable models of the structural perturbations induced by the ionization in doped polythiophene.

I. Introduction

The present development of the research of the π-conjugated materials offers the possibility of producing advanced materials which combine the electronic and optical properties of semiconductors and metals with the mechanical behavior and processing advantages of polymers. The key to the ultimate goal of designing suitable devices with the desired properties is the understanding of the structure−property relationship.[1,2] Solubility of the material is also of primary importance to ensure an easy and low cost of processing. The synthesis of various classes of stable oligomers with rigorously controlled substitution patterns and chain lengths is receiving considerable attention since it constitutes the most straightforward procedure to establish the precise structure−property relationships of these new materials.[3]

Doped π-conjugated polymers show high electrical conductivities, whereas undoped systems are either semiconductors or insulators. Among these conducting polymers, polythiophene has attracted considerable attention because of its excellent chemical stability and interesting electronic properties.[4−6]

The main process of chemical doping of π-conjugated materials is a redox reaction between the molecular backbone and electron acceptors (p-type doping) or electron donors (n-type doping). Charge injection generates in these systems different types of self-localized excitations.[7,8] Such excitations result from the coupling of the π-electron degree of freedom to the molecular structure of the one-dimensional system via the electron−phonon (e−p) interaction. The e−p interaction causes structural relaxation which results in a self-locatization of the electronic excitations around the local structural distortions along the polymer chain (over several rings with geometrical changes), giving rise to electronic states within the gap. Furthermore, the geometry of the charged excitations is believed to possess the quinonoid structure.[9]

We use here Raman scattering and infrared absorption spectroscopies to probe the fundamental modes of vibration of a series of α-coupled bithiophenes having a quinonoid structure in their electronic ground states, to get useful information on the geometrical modifications induced by charge carriers in doped polythiophene. In addition, these oligothienoquinonoids have been found to possess exceptionally large nonlinear hyperpolarizability $\langle\gamma\rangle$ as compared with the class of oligothienoaromatics.[10] Moreover, these compounds exhibit electron-acceptable properties as strong as those of the corresponding benzenoid quinodimethanes.[11]

The Raman spectra of π-conjugated materials show characteristic features, related to the degree of intramolecular delocalization of π-electrons along the molecular long axis, whose explanation has required the development of new theoretical concepts. One of the main challenges of the research of these oligomers is to investigate the relevant properties of extensively conjugated chains as a function of the "effective conjugation length", qualitatively defined as the length of the molecular domain over which π-delocalization takes place.

The major advantages of investigating this series of heteroquinonoid dimers can be summarized as follows. (i) The encapsulation of the end α-positions by dicyanomethylene groups produces additional extension of π-conjugation. (ii) The coexistence of an electron-rich moiety (the bithiophene spine in the present case) and an electron-deficient moiety (the dicyanomethylene groups on either side of the molecule) is expected to cause *intramolecular charge transfer*.[12] In this case, the wave function of the electronic ground state will involve a linear combination of (i) a charge-separated state and (ii) a nonpolar state.[13] The charge-separated counterpart of 2,2′-(2,2′,5,5′-tetrahydro-2,2′-bithienylidene-5,5′-diylidene)bis(propanedinitrile) (referred to as Th2CN4 henceforth) comprises a positively charged bithiophene backbone and the dicyanomethylene end caps (and their vicinity) charged negatively. Thus, the structure of these bithienoquinonoids most likely represents the charged species induced by chemical doping in polythiophene and oligothiophenes.

II. Experimental Section

The chemical structures and atom numberings of Th2CN4 and their three β-dihexyl regioregular isomers are plotted in Figure 1. The synthesis of these bithienoquinonoids is reported

[†] Universidad de Málaga.
[‡] Toyama University.

10.1021/jp993812u CCC: $19.00
Published on Web 12/30/1999

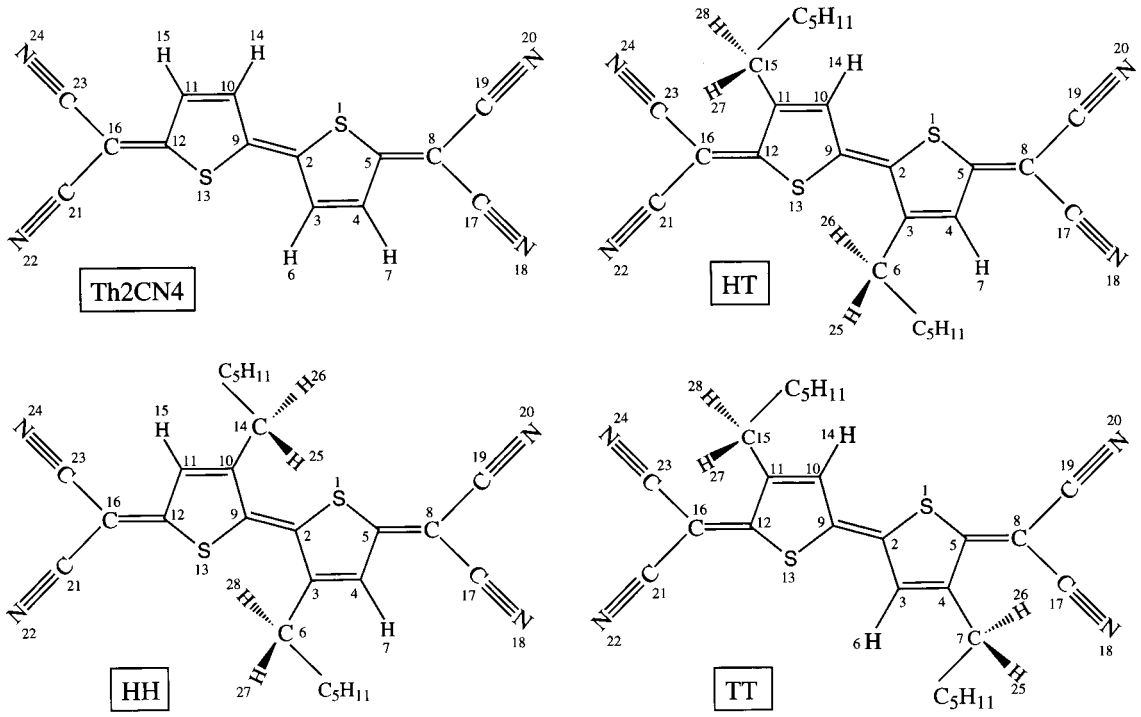

Figure 1. Chemical structures and atom numberings of the compounds studied in this work.

elsewhere.[14] The $\pi-\pi^*$ absorption maximum of Th2CN4 (measured in the form of a thin film deposited onto a quartz substrate) is located at 527 nm.[15] On the other hand, the electronic absorption spectra of the regioregular head-to-head (HH), head-to-tail (HT), and tail-to-tail (TT) β-dihexyl bithienoquinonoid isomers were recorded in dichloromethane solution.[14] The main absorption bands for these compounds are as follows: 554 nm (HH), 541 nm (HT), and 554 nm (TT). These data can be compared with those for the corresponding series of β-dihexyl bithienoaromatics (measured also in CH_2Cl_2 solution): 247 nm (HH), 297 nm (HT), and 311 nm (TT).

In the heteroaromatic series of compounds, the variable position of the $\pi-\pi^*$ band can be attributed to the degree of deviation from coplanarity by twisting of the rings due to the steric repulsion between the hexyl substituents and the sulfur atoms belonging to the opposite thiophene rings. The large bathochromic shift of the $\pi-\pi^*$ transition in going to the heteroquinonoid series clearly reflects the highly extended π-electron conjugation of this class of materials. This redshift can also be in part attributed to the electron-withdrawing ability of the α-dicyanomethylene end caps. We observe however that, in the bithienoquinonoids, the position of the $\pi-\pi^*$ band varies very little from one isomer to another. In other words, it can be concluded that the orientation of the two constituent 3-hexylthiophene units does not affect the electronic structure for a bithienoquinonoid chromophore so much as for a 2,2′-bithienoaromatic chromophore, and thus all these bithienoquinonoids are expected to be substantially planar molecules.

The infrared absorption spectra were recorded in the form of pressed KBr pellets with a Perkin-Elmer FT-IR spectrometer model 1760 X purged with dry Ar gas. The spectra were measured in the 400−4000 cm^{-1} frequency range at room temperature, and 20 scans with 2 cm^{-1} spectral resolution were accumulated. The FT-Raman spectra were collected at room temperature on a Bruker FRA106/S FT-Raman spectrometer in a backscattering configuration. We used as an exciting line the 1064 nm radiation of a Nd:YAG laser. To avoid local degradation of the compounds, the laser beam power was limited to 10 mW and 1000 scans, with 2 cm^{-1} spectral resolution, were added to increase the signal-to-noise ratio.

III. Computational Details

The ability to calculate molecular force fields and geometries for both closed- and open-shell systems is one of the greatest achievements in computational chemistry over the past decade. Most calculations are carried out in the ab initio Hartree−Fock (HF) scheme. At this level, the calculated harmonic force constants and frequencies are usually higher than the corresponding experimental values, due to a combination of electron correlation effects and basis set deficiencies. As the errors in the calculations are largely systematic, they can be corrected after inclusion of appropriate scaling factors.

However, the HF method fails to give proper qualitative descriptions for systems when nondynamical electron correlation is of primary importance. This category of systems is found among molecules with multiple bonds as well as open-shell species. Density functional theory (DFT) is an alternative approach for adding electron correlation, and its computational requirements are comparable to those for the HF method.[16,17] DFT calculations provide harmonic vibrational frequencies of similar accuracy to the MP2 results.[18,19]

DFT calculations were performed with the Gaussian 94 program[20] on a SGI Origin 2000 supercomputer, by using the B3LYP functional.[21] It has been shown that the B3LYP functional yields similar geometries and vibrational properties for medium-sized systems as MP2 calculations do with the same basis sets.[18,19,22,23] We have used throughout the work the split valence 6-31G** basis set, which includes a set of d-polarization functions for heavy atoms and p-polarization functions for hydrogens.[24]

The geometry optimizations were performed on isolated entities, with the only constraint of keeping the inversion center for the Th2CN4 molecule, and the HH and TT isomers. Geometrical parameters were allowed to vary independently but with the constraint that a fully planar, anti configuration was

retained for the thiophene rings. The required computer time is comparatively larger for the HT isomer due to the absence of internal symmetry. Thus, we decided to mimic the β-alkyl substitution with a propyl group, as a good compromise between feasibility of calculations and reliability of results. Under these assumptions, the Th2CN4 and the HH and TT isomers have C_{2h} symmetry, whereas the HT isomer displays C_s symmetry.

Harmonic vibrational frequencies and infrared intensities were calculated analytically on the optimized geometries. We recall that Gaussian 94 does not give the Raman activities for DFT calculations so that it is not possible to report on the calculated Raman spectral profiles. Nonetheless, useful information can be derived from the inspection of the theoretical eigenvectors.[25] We have made use of an often-practiced simple adjustment of the theoretical force fields in which frequencies are scaled down uniformly by a factor of 0.96, as recommended by Scott and Radom.[19] This procedure is advisable for large-scale studies because it avoids the fairly complex definition of the internal coordinates. All quoted vibrational results are thus scaled values.

To shed further light on the electronic modifications on the systems upon substitution, we have performed an analysis of the electronic charge density within the framework of the theory of atoms in molecules developed by Bader.[26] The MORPHY1.0[27] and the AIMPAC[28] suite of programs have been employed for that purpose. Let us briefly outline the theory of atoms in molecules for the benefit of the reader. The topology of the electronic charge density, $\rho(\mathbf{r})$, exhibits critical points (CP) that can be classified by the number of the nonzero curvatures (λ_1, λ_2, λ_3) of the Hessian matrix evaluated at the CPs (i.e., the *rank*) and the algebraic sum of their signs (called the *signature*). Hence, four types of CPs can be found, namely: maxima (3,−3), saddle (3,−1), and (3,+1), and minima (3,+3) CPs. These points are usually associated with structural elements present in the molecule: nuclei, bonds, rings, and cages, respectively. The sum of the curvatures is the Laplacian of the charge density, $\nabla^2\rho(\mathbf{r})$, which indicates the degree of local concentration of charge. The number of CPs fulfills the Poincaré−Hopf relationship: nuclei − bonds + rings − cages = 1. The gradient vector field of the charge density, $\nabla\rho(\mathbf{r})$, links (through its trajectories) the different CPs of $\rho(\mathbf{r})$ and defines the atom within the molecule, the bond paths, and hence the molecular graph.

In particular, we shall pay attention to the amount of the charge density, ρ_b, and to the sign and magnitude of the Laplacian of the charge density, $\nabla^2\rho_b$, at the bond critical points (BCP), since these quantities enable one to classify the atomic interactions.[26] Typical shared interactions exhibit large amounts of both $\rho(\mathbf{r})$ and $\nabla\ ^2\rho(\mathbf{r})$ at the BCPs, and the Laplacian is negative. Closed-shell interactions (such as vdW ones) present low values of ρ_b and $\nabla^2\rho_b$, the latter being positive. Between them, the intermediate bonding interactions exhibit large values of ρ_b and $\nabla^2\rho_b$, but the Laplacian in this case is positive as a consequence of the great value that attains the eigenvalue in the direction of the bond path (λ_3). The ellipticity, ϵ, of the charge density at the BCPs is defined as $\epsilon = (\lambda_1/\lambda_2) - 1$, where λ_1 and λ_2 are the eigenvalues of the Hessian matrix of $\rho(\mathbf{r})$ corresponding to the eigenvectors perpendicular to the bond path. This magnitude provides a measure of the accumulation of the charge density in a particular plane. In this work, the charge densities were constructed from B3LYP/6-31G**// B3LYP/6-31G** wave functions. Equilibrium atomic charges were computed using natural population analysis[29] of the corresponding density matrices. All magnitudes are in atomic units unless otherwise noted.

TABLE 1: B3LYP/6-31G Optimized Bond Lengths (in Å) for the Skeletal Bonds for Th2CN4 and the Symmetric Isomers**

bond	Th2CN4	HH	TT
S_1-C_2	1.779	1.791	1.770
S_1-C_5	1.761	1.751	1.768
C_2-C_3	1.436	1.466	1.430
C_3-C_4	1.361	1.366	1.368
C_4-C_5	1.439	1.429	1.458
C_5-C_8	1.382	1.384	1.385
C_8-C_{17}	1.425	1.425	1.427
C_8-C_{19}	1.425	1.425	1.427
$C_{17}-N_{18}$	1.165	1.165	1.165
$C_{19}-N_{20}$	1.165	1.165	1.165
C_3-H_6[a]	1.084	1.511	1.083
C_4-H_7[b]	1.083	1.082	1.510
C_2-H_9	1.375	1.382	1.375

[a] This C−H bond is a C−C single bond for the HH isomer. [b] This C−H bond is a C−C single bond for the TT isomer.

IV. Results and Discussion

A. Optimized Geometries, Natural Bond Orbital Atomic Charges, and Charge Density. Table 1 and Table 1S (in the Supporting Information) summarize the main skeletal bond lengths and the natural bond orbital atomic charges, respectively, for the Th2CN4 molecule and the HH and TT isomers. All optimized geometries are compatible with the attainment of a heteroquinonoid structure. Taking the Th2CN4 as the prototypical case, the effects on the molecular parameters of the π-conjugated backbone of the three different β-alkyl substitution patterns can be summarized as follows.

(i) In the HH isomer, the geometrical changes are with great probability due to the repulsive electrostatic interactions between the sulfur atom and the two nearest hydrogen atoms of the alkyl side chain (S_1, + 0.46; H_{25} and H_{26}, + 0.27). These interactions are partially compensated by the attractive interaction with the alkyl C atom directly attached to the thiophene ring, due to the existence of the opposite sign charge density over this last atom (C_{14}, −0.50). Nonetheless, looking solely at the natural charges on heavy atoms, we find that the net electrostatic interaction between the sulfur atom and the first methylene group is slightly attractive. The increased steric hindrance caused by this interaction could justify the lengthening of the inner C_2-C_9, C_2-C_3, and C_2-S_1 bonds by about 0.007, 0.030, and 0.012 Å, respectively. The elongation of these bonds are accompanied by the shortening of both the outer C_4-C_5 and C_5-S_1 bonds by about 0.010 Å.

(ii) In the optimized geometry of the TT isomer, we notice that only the outer C_4-C_5 bond undergoes an appreciable lengthening by about 0.020 Å, while the remainder bond lengths vary very little. These changes are likely the result of the balance of the electrostatic interactions and steric effects between the alkyl chain and the dicyanomethylene moiety. The electrostatic interaction between the charge on the first methylene group (C_7, −0.49) and the nearest carbon atom of the dicyanomethylene end-cap (C_{17}, +0.26) has an attractive character.

(iii) The situation for HT isomer is halfway between that of the HH isomer and the TT isomer. Thus, the geometrical changes are almost the simple superposition of the effects induced by the β-substitution on the isolated 3-alkyl and the 4-alkyl constituent thienyl moieties. That is, (a) in the 4-alkyl substituted thiophene ring, only the outer $C_{11}-C_{12}$ bond experiences a significant lengthening by about 0.018 Å, while (b) in the 3-alkyl substituted thiophene ring, both the inner C_2-C_3 and C_2-S_1 bonds lengthen by about 0.018 and 0.006 Å,

respectively, and both the outer C_4-C_5 and C_5-S_1 bonds undergo a shortening by about 0.007 Å with respect to the Th2CN4.

The information derived from the B3LYP/6-31G** calculations is that the substitution of the hydrogen atoms at the β-positions of the Th2CN4 by alkyl chains does not translate only into molecular geometry changes, but also the natural atomic charges supported by the C atoms of the heteroquinonoid skeleton are affected. Particularly, the charge on the C_β atom attached to the alkyl chain largely increases from -0.20 or -0.22 in Th2CN4 up to $+0.02$ in the 3-alkyl unit and -0.01 in the 4-alkyl unit. This induces a partial polarization of the double $C_\beta = C_\beta$ bonds upon alkylation. Small changes in the equilibrium atomic positions of a molecule are known to have little influence on its vibrational spectrum. On the other hand, the changes in the equilibrium charge distribution and the charge mobility during normal vibrations greatly affect the infrared intensity pattern. Different models have been proposed in the past which allow useful parameters related to the electronic structure of molecules to be derived from experimental infrared intensity data. The best known and most widely used parameters are the APT (atomic polar tensors),[30] EOP (electrooptical parameters),[31] and ECCF (equilibrium charges and charge fluxes).[32]

The analysis of the charge density for the systems under study rendered 45 bond critical points (BCP) together with 4 ring critical points (RCP), so fulfilling the Poincaré−Hopf fomulas. The values of the properties related to the charge density (ρ_b, $|\nabla^2\rho_b|$, $|\lambda_1|$, $|\lambda_2|$, λ_3, and ϵ) at the BCPs of the four systems are summarized in Table 2S in the Supporting Information.

First, one observes the high values of ϵ for all the bonds of the backbone so confirming the π-delocalization previously noted (for instance, the triple $C_{17}\equiv N_{18}$ bond exhibits a close-to-zero value because of the cylindrical symmetry of the charge density around the bond, and hence $\lambda_1 \approx \lambda_2$).

In general, from the variation in the eigenvalues (in going from the HH to the TT isomers), one sees that a smaller amount of the charge density at the BCP is due to migration of $\rho(r)$ from the perpendicular planes to the bond path towards the nuclei. Thus, $|\lambda_1|$ and $|\lambda_2|$ diminish (and hence the ellipticity ϵ), whereas λ_3 grows.

Interestingly, two unexpected ring structures appear as a consequence of closed-shell interactions (ρ_b amounts to 0.0130 and $\nabla^2\rho_b$ to 0.0523 for the HH isomer, and $\rho_b = 0.0096$ and $\nabla^2\rho_b = 0.0378$ for the TT isomer) between (i) the first alkyl-C atom and the sulfur atom of the adjacent ring, in the HH and HT isomers, and (ii) the first alkyl-C atom and the carbon atom of the nearest CN group, in the HT and TT isomers. These interactions were anticipated in view of the charges of the atoms involved. The gradient vector field of $\rho(\mathbf{r})$, $\nabla\rho(\mathbf{r})$, is plotted for the planes of interest in the case of HT isomer in Figures 2 and 3. Although the bond paths are not actually plotted, the ridges connecting C_{15} and C_{23} atoms (Figure 2) and C_6 and S_{13} atoms (Figure 3) can be observed. These interactions could be the origin for the remarkable enhancement of the infrared-active vibrations above 1400 cm^{-1} of the three β-substituted isomers with respect to the spectral pattern of the Th2CN4 (see below).

The comparison of the values of ρ_b, $|\nabla^2\rho_b|$, $|\lambda_1|$, $|\lambda_2|$, λ_3, and ϵ for a given bond along the whole series of compounds (Table 2S) reveals different trends of variation depending on the position of the bond within the molecule. We assume that the HT isomer is an intermediate situation between the HH and TT systems and therefore it will be not given any comment on its features.

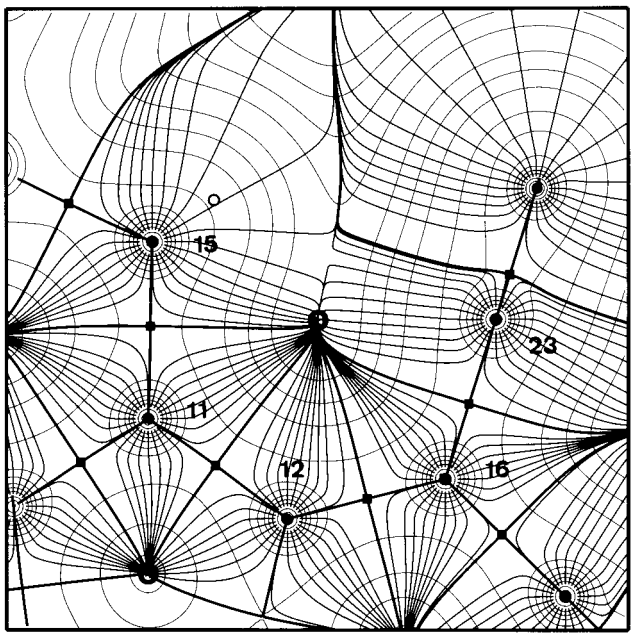

Figure 2. Gradient vector field and contour map of the charge density for the HT isomer in the plane defined by the ring critical point and the C_{15} and C_{23} nuclei.

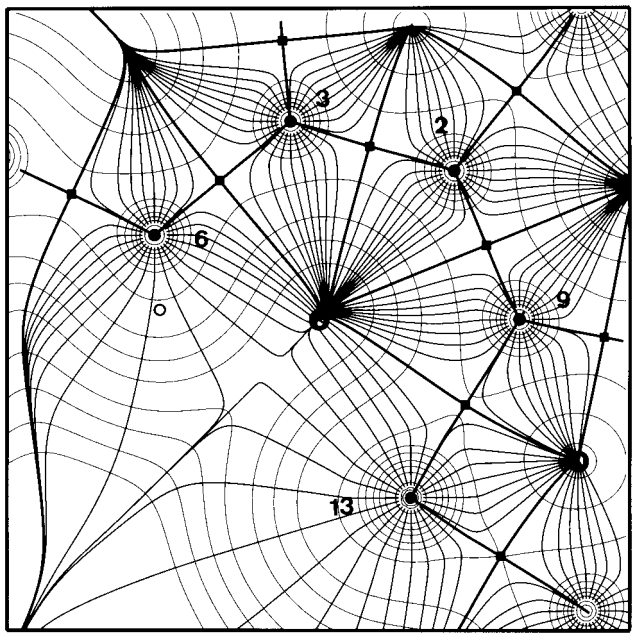

Figure 3. Gradient vector field and contour map of the charge density for the HT isomer in the plane defined by the ring critical point and the C_6 and S_{13} nuclei.

Let us first comment on the central double bond of the molecule. The maximum ρ_b and the absolute value of its associated Laplacian, $|\nabla^2\rho_b|$, are attained for Th2CN4. Upon substitution in a head-to-head orientation, the values decrease, especially the Laplacian, and grow again upon substitution in tail-to-tail orientation, reaching values close to the maxima. Hence, the central double bond is expected to show a similar behavior for Th2CN4 and the TT isomer. The variation of the ellipticity follows a different trend, increasing from Th2CN4 to the HH isomer and attaining its minimum value for the TT isomer. The bonds attached to the central double bond exhibit a similar pattern of variation for ρ_b and $|\nabla^2\rho_b|$. Notably, the Laplacian for the adjacent C−C ring single bond (C_2-C_3 in Th2CN4) decreases in a large amount for HH, attaining the

TABLE 2: Distribution of the Normal Modes in the Various Symmetry Species for the Oligomers with Molecular C_{2h} Symmetry

mode symmetry	optical activity	Th2CN4	HH	TT
	in-plane modes			
Ag	(Raman pol.)	23	53	53
Bu	(IR)	22	52	52
	out-of-plane modes			
Au	(IR)	11	35	35
Bg	(Raman depol.)	10	34	34

TABLE 3: Distribution of the Normal Modes in the Various Symmetry Species for the Oligomer with Molecular C_s Symmetry

mode symmetry	optical activity	HT
	in-plane modes	
A′	(IR, Raman)	105
	out-of-plane modes	
A″	(IR, Raman)	69

maximum for TT, being the ellipticity the greatest for this isomer too. The adjacent C−S bond (C_2-S_1 in Th2CN4) exhibits similar changes, although for the TT isomer the ellipticity is not a maximum.

The values of ρ_b and $|\nabla^2\rho_b|$ for the ring double bonds (i.e., C_3-C_4 and $C_{10}-C_{11}$ in Th2CN4) decrease monotonically, attaining the minima values for the TT isomer. A similar trend of variation is found for the outermost double bonds and the C−C single bonds linking them with the two CN groups (i.e., C_8-C_{17}, and C_8-C_{19} in Table 2S) except for the ellipticity at the BCPs, which grows upon substitution in tail-to-tail orientation, indicating that more π-density is placed at the BCP.

Similar changes in ρ_b and related properties for the central double bond and its neighborhoods lead us to think that these are caused by the new ring structure formed as a consequence of the closed-shell interaction between the sulfur and the first alkyl-C atom of the propyl group. The same can be said for the external double bond, but now caused by the interaction between the propyl and the carbon atom of the CN group. Therefore, the amount of charge density in the bonds that form the new ring structures decreases in order to accommodate the new interactions between the first alkyl-C atom and the nitrile-C and S atoms, respectively, thus, mirroring the elongation in the bond distances discussed above.

B. Structure and Selection Rules. No experimental X-ray or electron diffraction data are available for the Th2CN4 molecule and its three β-dialkyl derivatives. The X-ray structures of related heteroaromatic compounds (such as unsubstituted α-oligothiophenes[33] and α,α′-dimethyl end-capped quaterthiophene[34]) have shown that the small steric and electrostatic interactions between the hydrogens at the 3-position and the sulfur atom in the neighboring thiophene unit serves for the alignment of the rings in a fully coplanar transoid disposition. Moreover, in our heteroquinonoids, the possibility of rotation around the bond connecting the two rings is highly restricted due to its double bond character. So that, in agreement with the constant position of the $\pi-\pi^*$ electronic transition for the three regioregular isomers, we can reliably assume that all the molecules are essentially planar systems. The distribution of the vibrational normal modes in the various symmetry species for each material is shown in Tables 2 and 3.

Although the selection rules predict a very large population of bands in the infrared and Raman spectra (up to 174 in the HT isomer), the actual spectra are surprisingly simple. This seeming discrepancy between the theoretical predictions and the experimental spectra may be in part due to the following considerations.

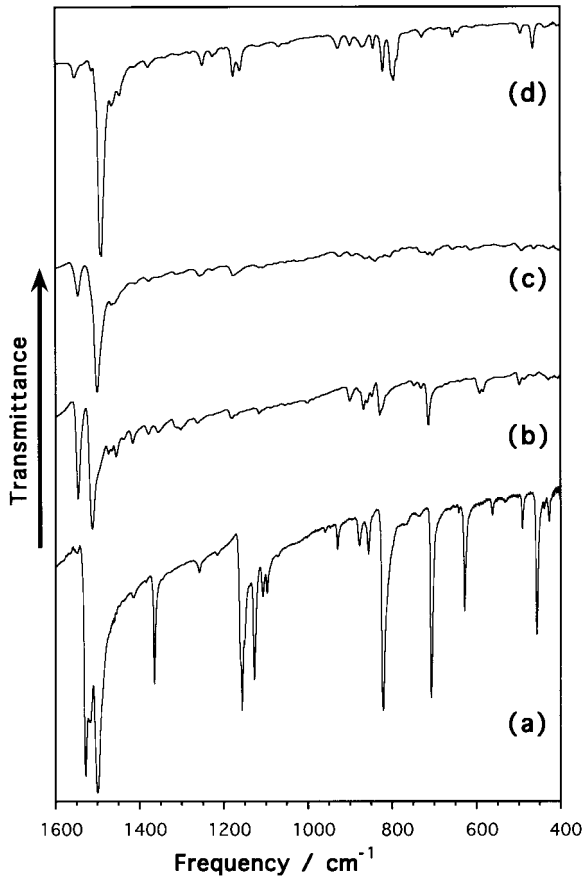

Figure 4. FT-IR spectra of Th2CN4 (a) and of the HH (b), HT (c), and TT (d) regioregular isomers in the 1600−400 cm^{-1} spectral range.

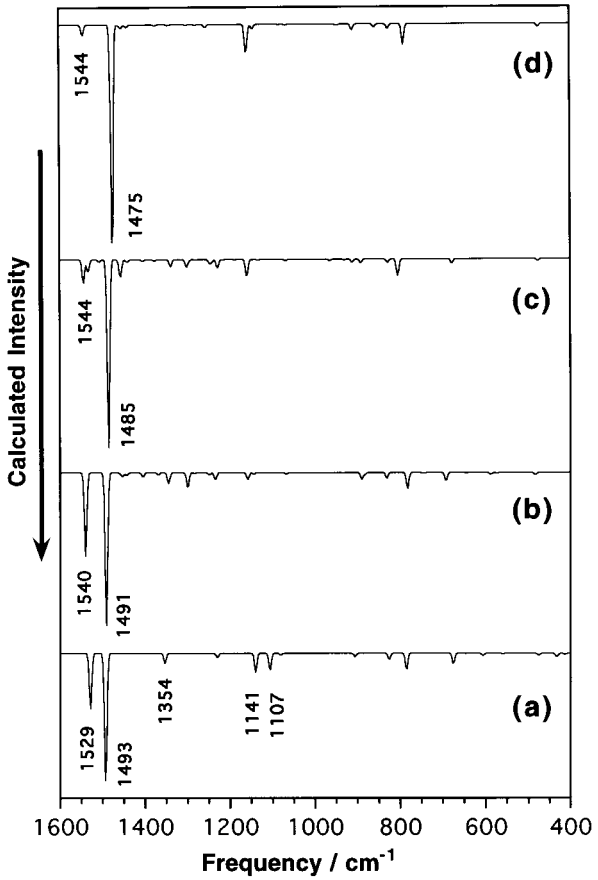

Figure 5. Theoretical (B3LYP/6-31G**) infrared spectra of Th2CN4 (a) and of its three HH (b), HT (c), and TT (d) regioregular isomers in the 1600−1000 cm^{-1} spectral range.

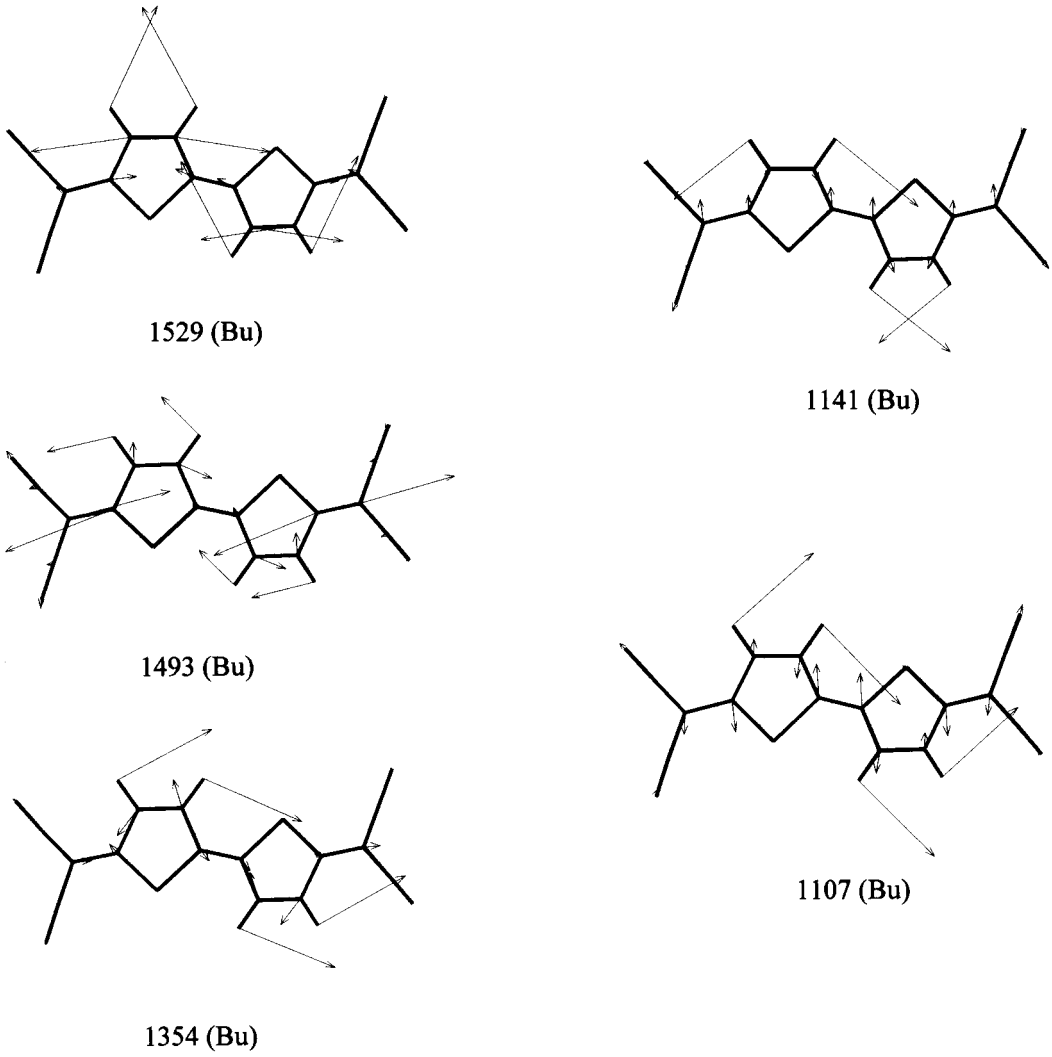

Figure 6. Schematic eigenvectors for the most intense infrared vibrations of the Th2CN4 molecule calculated at the B3LYP/6-31G** level (scaled values are given in cm^{-1}).

(1) Since the two dicyanomethylene caps attached to the terminal α positions are relatively far apart, no mechanical coupling is expected to take place between their characteristic vibrations. Therefore, we expect that both their in-plane and out-of-plane motions are degenerate and do not show any splitting in the spectra.

(2) Vibrations of groups with a strong local character can also be scarcely coupled with the neighbor oscillators, their frequencies being almost independent of the phase angle. This should be the situation for the aromatic and aliphatic C−H stretchings and bendings modes.

(3) As resonance Raman is approached,[35] a few Raman lines are known to gain much intensity relative to all other Raman active normal vibrations. When the molecular symmetry does not change from the ground to the excited state, only totally symmetric vibrations are resonance enhanced.

C. Infrared Spectra. The FT-IR spectra of Th2CN4 and the three HH, HT, and TT isomers in the 3500−2000 and 1600−400 cm^{-1} spectral ranges are displayed in Figure 1S (in the Supporting Information) and Figure 4, respectively. A general rising of the absorption is observed for all the compounds on the higher energy side of the spectrum. This feature represents the tail of the absorbance of the $\pi-\pi^*$ transition in the near-infrared region.[15]

The C≡N stretching vibration is measured as a medium-strong band near 2213−2215 cm^{-1} for all the compounds. The shift toward lower frequencies of this vibration on complexation with electron donors has been related to the degree of charge transfer in organic conductors.[36] As aforementioned in the Introduction, the coexistence in these materials of a central electron-rich bithiophene moiety and two electron deficient dicyanomethylene end caps is expected to cause *intramolecular charge transfer*.[12]

The degree of the intramolecular charge transfer (ρ) can be estimated to be about 0.28 on the basis of Figure 1 of ref 36, which shows the relationship between ρ and the C≡N stretching vibration frequencies for various TCNQ salts. This value can be compared with that obtained for the unsubstituted heteroquinonoid trimer Th3CN4 of about 0.4.[37] The constant magnitude of ρ for the four compounds is in agreement with the theoretical finding that the β-alkylation of the π-conjugated spine does not modify to a large extent the atomic charges on the dicyanomethylene end-caps with respect to the unsubstituted system.

As can be seen in Figure 4, the spectrum of Th2CN4 is characterized by the appearance of a number of sharp absorptions spreading over the whole spectral range. On the contrary, the spectra of the β-hexyl substituted isomers show only two main bands, centered at around 1550 and 1500 cm^{-1}. The intensity patterns of the four compounds are nicely reproduced, at least above 1000 cm^{-1}, in the B3LYP/6-31G** theoretical spectra (see Figure 5). The complete assignment of the infrared

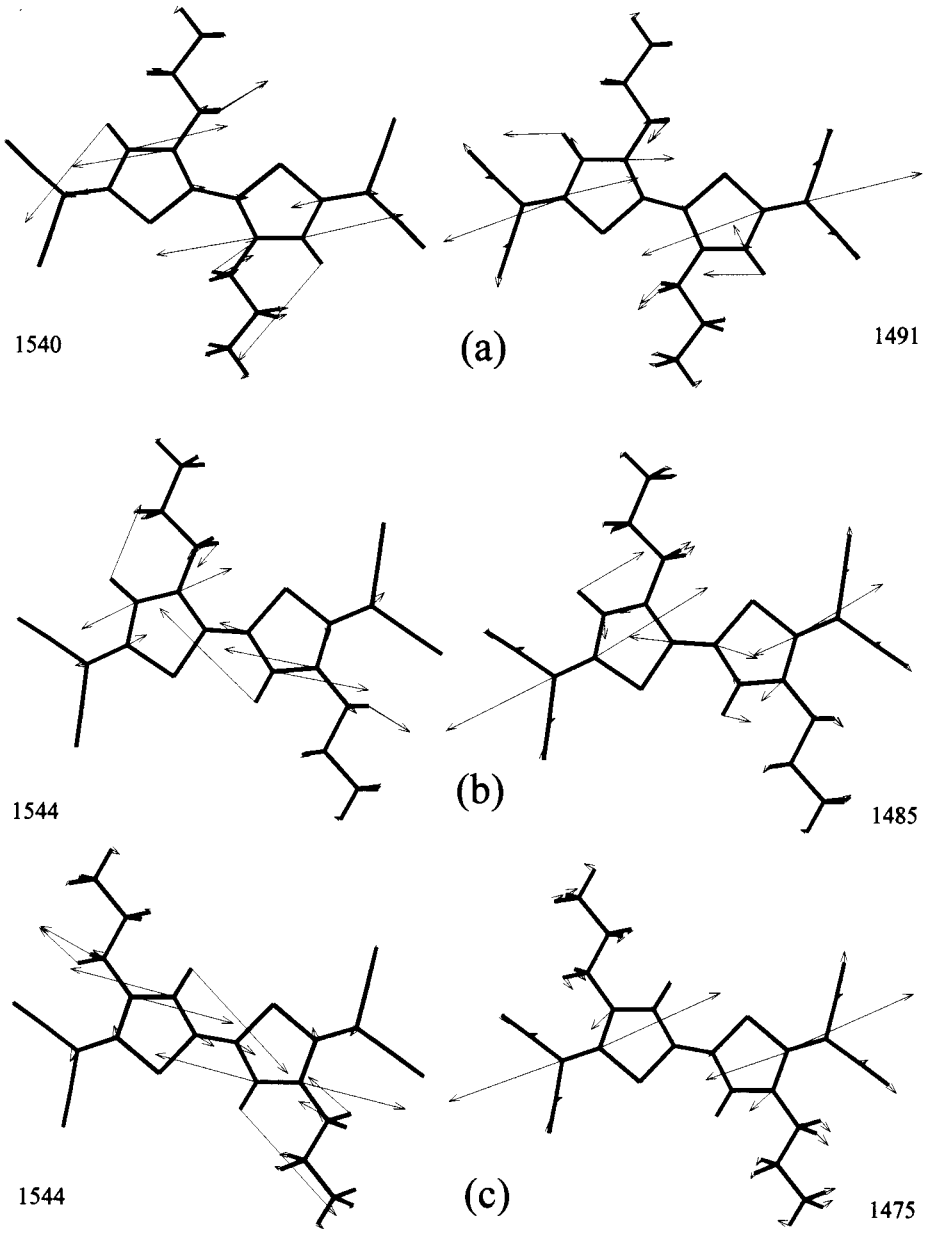

Figure 7. Schematic B3LYP/6-31G** eigenvectors for the infrared bands near 1550 and 1500 cm^{-1} of the HH (a), HT (b), and TT (c) isomers.

bands of each oligomer to particular vibrations is beyond the scope of this work. Nonetheless, meaningful structural information can be gathered from the inspection of the spectra. Another difference between the infrared spectrum of Th2CN4 and those of its β-hexyl substituted isomers is that in the latter the bands appear as rounded features, their spectra being much more similar to that recorded for Th3CN4.[37] These differences may be due to the positive inductive effect by the alkyl groups. As deduced from the B3LYP/6-31G** calculations, the β-alkylation promotes an injection of charge toward the conjugated skeleton (see Table 1S of the Supporting Information). That is to say, in the Th2CN4 molecule the overall charge on each thiophene unit (with hydrogens summed into heavy atoms) is + 0.26, whereas it goes down to about +0.21 in the three regioregular isomers.

The atomic vibrational displacements for the most intense infrared bands of Th2CN4 and the HH, HT, and TT isomers, calculated at the B3LYP/6-31G** level, are sketched in Figures 6 and 7. Analyzing the data (compare Figures 4 and 5), we find that by far the largest contributions stem from the CC bond stretching along the polyconjugated chain. The most intense peaks for Th2CN4 are calculated at 1529 (exp. 1528) and 1493 (exp. 1499) cm^{-1}. These absorptions correspond to the almost pure antisymmetric stretchings of the $C_\beta = C_\beta$ and the $C_\alpha = C_{sp2}$ bonds, respectively. The peak at 1354 (exp. 1365) cm^{-1} arises from the antisymmetric stretching of the two $C_\alpha - C_\beta$ bonds of each ring, for which the vibrational motions of both thiophene units take place in out-of-phase. Finally, the peaks at 1141 (exp. 1156) and 1107 (exp. 1127) cm^{-1} are due to the symmetric and antisymmetric in-plane bendings of the C−H bonds attached to the rings; also, in this case the symmetry-equivalent oscillators vibrate in out-of-phase.

The theoretical eigenvectors for the HH, HT, and TT isomers support the assignment of the bands near 1550 and 1500 cm^{-1}, as for the Th2CN4 molecule, to the antisymmetric stretchings of the $C_\beta = C_\beta$ and the $C_\alpha = C_{sp2}$ bonds, respectively. The upshift by 10−15 cm^{-1} of the former band in the three isomers with respect to Th2CN4 is likely the result of a mass effect on the kinetic G matrix[38] due to the substitution of a hydrogen atom by a bulky alkyl chain. However, the different position of the absorption near 1500 cm^{-1} cannot be attributed to modifications on the G matrix only, but to the changes induced by the presence of the alkyl side chain on the electronic charge

density, $\rho(\mathbf{r})$, of the outermost C=C double bond. As a result of the aforementioned closed-shell interactions between the first alkyl-C atom (C_7) and the $C_{17}(\equiv N)$, the vibration associated with the absorption of the TT isomer at 1490 cm^{-1} (calculated at 1475 cm^{-1}) is strongly localized in the vicinity of the $C_\alpha = C_{sp2}$ bonds. On the contrary, the absence of these interactions in the HH isomer, extends the atomic displacements beyond the external double bonds up to the central double bond, which hardly vibrates because of the interactions between the first alkyl-C atom and the sulfur atoms. Precisely, the rigidity provoked by these new interactions in HH makes the vibration more difficult, bringing the frequency up to 1511 cm^{-1} (calculated at 1491 cm^{-1}). Moreover, the charge density decrease (as measured at the BCPs) in the bonds surrounding the external closed-shell interactions in the TT isomer (and in the T-side of HT) accounts for the downshift of its frequency.

On the other hand, the high-frequency vibration (i.e., 1550 cm^{-1}) is practically the same for the three isomers, since the corresponding eigenvectors are equivalent and the external and internal closed-shell interactions play parallel roles in fixing the movement of the first methylene group of the alkyl side chain. Precisely, the doublet observed in the HT isomer can be due to the slight difference between the two types of closed-shell interactions. Finally, we observe that the intensity of the band at 1550 cm^{-1} relative to that at 1500 cm^{-1} readily decreases in the order HH > HT > TT. The theoretical spectra displayed in Figure 5 also show a similar trend. The calculated intensity values for these bands in the three isomers are the following: HH (350 and 640 km mol^{-1}); HT (98 and 784 km mol^{-1}); TT (44 and 997 km mol^{-1}).

D. Raman Spectra. The FT-Raman spectra of Th2CN4 and its three isormers are shown in Figure 8. The four spectra are rather similar both in band positions and relative intensities. Moreover, the spectra display very few bands, despite the very large population of bands predicted by the optical selection rules (see Tables 2 and 3). The last observation results from the selective enhancement of particular totally symmetric normal vibrations associated with the electron−phonon interaction characteristic of these π-polyconjugated materials.[39−43]

These features are not solely due to the proximity of the exciting laser to the molecular energy gap[35] but also to the main role played, even if the resonance condition is not fulfilled, by *only one* strongly dipole-allowed electronic excited state in the Raman process. These particular phenomena have been already explained for polyacetylene by the amplitude mode theory of Horovitz[44] and more recently in molecular dynamics terms, for many classes of polyconjugated polymers, by the effective conjugation coordinate (ECC) theory. We refer the reader to the existing literature for a presentation of the basic concepts of the ECC theory.[45−48]

Ab initio Hartree−Fock vibrational calculations performed in the past few years on some closed-shell oligothiophenes (in the form of neutral[49] and dicationic[50] species) further support, in full accordance with the predictions of the ECC theory, that the most intense Raman scatterings are exclusively due to totally symmetric normal vibrations. Unfortunately, the Gaussian 94 package[20] does not provide the Raman activities for DFT calculations. As a consequence, no theoretical Raman spectrum can be calculated within the DFT scheme. Despite these limitations, meaningful information can still be derived from the correlation between scaled and experimental frequencies and from the theoretical eigenvectors associated with the totally symmetric molecular modes. As an aid for the assignment of the Raman spectra, Table 4 summarizes the scaled B3LYP/6-31G** frequencies for the main totally symmetric modes (A_g or A_1 symmetry) of the four systems, while Figures 9 and 10 sketch the corresponding eigenvectors.

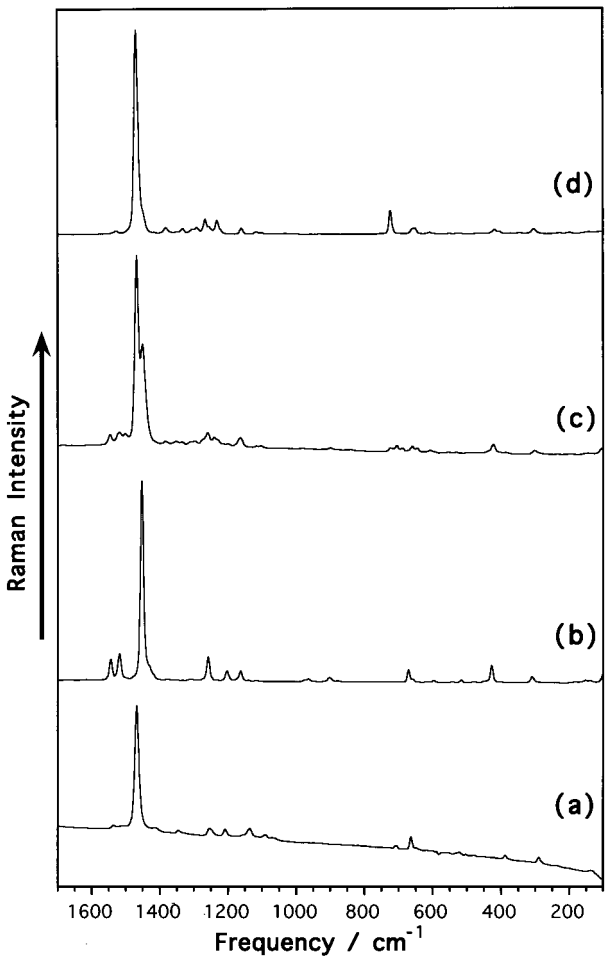

Figure 8. FT-Raman spectra of Th2CN4 (a) and of the HH (b), HT (c), and TT (d) regioregular isomers in the 1700−100 cm^{-1} spectral range.

TABLE 4: Correlation between the Calculated totally Symmetric Modes in the 1600−1000 cm^{-1} and the Experimental Values for the Four Systems Studied in This Work

Th2CN4		HH		HT		TT	
calcd	exptl	calcd	exptl	calcd	exptl	calcd	exptl
1536	1536	1540	1543	1533	1546		
1502	1510	1499	1518	1506	1519	1522	1528
1466	1468	1458	1453	1458	1468	1456	1470
				1448	1451		
1229	1255	1247	1259	1247	1261	1236	1268
1184	1209	1232	1204	1229	1241	1203	1233
1118	1138	1177	1164	1189	1164	1136	1162
1070	1092						

The Raman spetrum of Th2CN4 consists of a major line in the ring stretching region at 1468 cm^{-1}, accompanied by a number of very weak lines at 1536, 1510, 1413, 1346, 1255, 1209, 1138, 1092, 707, 664, 388, and 290 cm^{-1}. The very large Raman activity of the line at 1468 cm^{-1} indicates that it arises from a ν(C=C) vibration which largely matches the *ground electronic state−first electronic excited state minimum geometry* structural changes.[45−48]

We would like to remark that the Raman spectral pattern of the Th2CN4 *bithienoquinonoid* compound is halfway between those previously reported for a *heteroaromatic* series of α,α′-

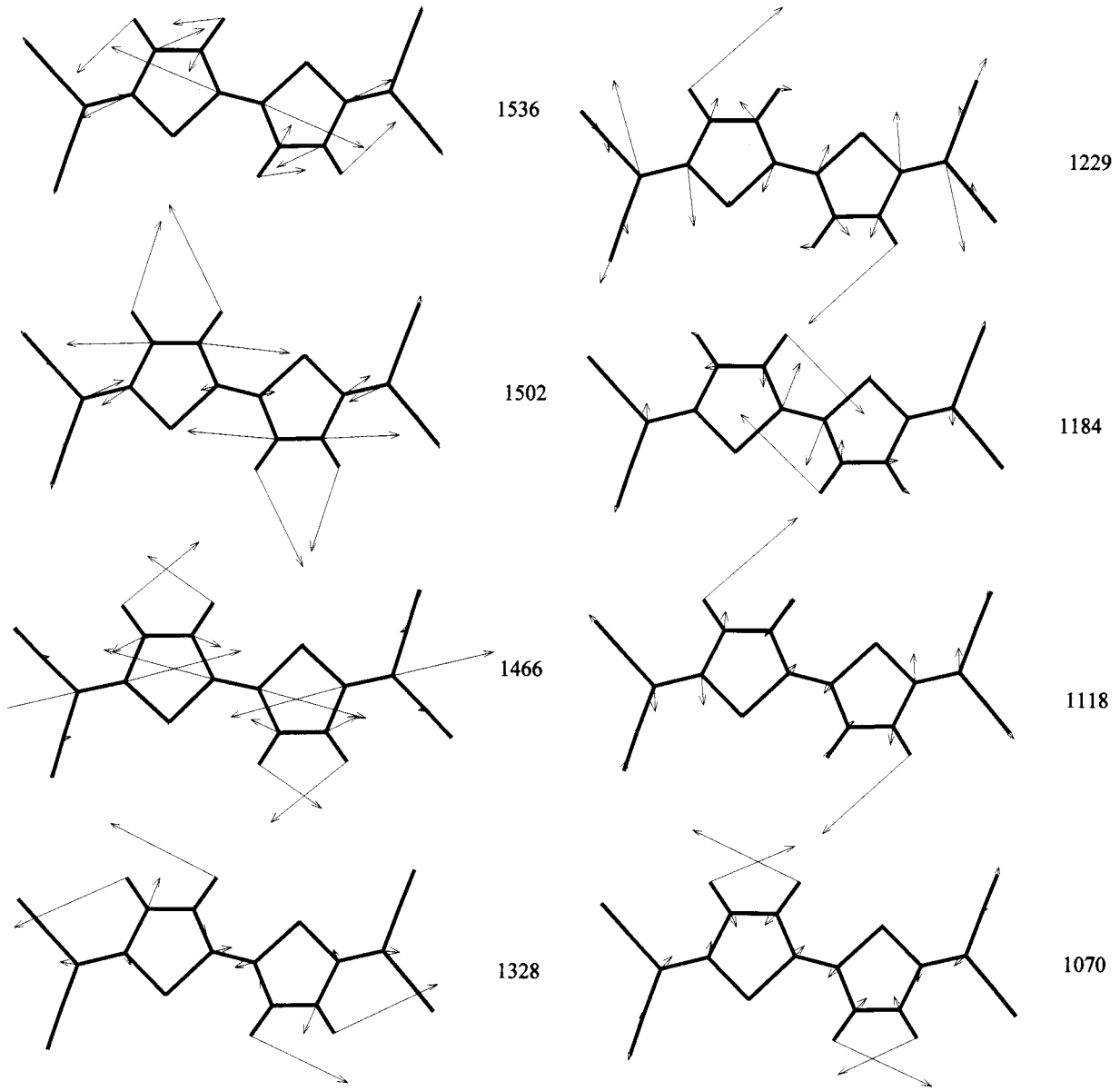

Figure 9. Schematic eigenvectors for some totally symmetric vibrations of the Th2CN4 molecule calculated at the B3LYP/6-31G** level (scaled values are given in cm^{-1}).

dimethyl end-capped oligothiophenes in the neutral state[43,51] and those of their corresponding radical cations (which are characterized by the appearance of a quinonoid defect in the middle of the molecule).[25] The main differences between the spectra of Th2CN4 and of the neutral form of the α,α′-dimethyl end-capped bithiophene[51] are (i) the appreciable enhancement of lines at 1468, 1346, 1255, 1209, and 1138 cm^{-1} in Th2CN4 and (ii) lines associated with stretching vibrations of the double C═C bonds (i.e., those appearing in the 1600−1400 cm^{-1} range) undergo a sizable shift downward by about 20−30 cm^{-1} upon quinoidization of the bithiophene backbone. These spectral differences resemble the changes observed in the Raman spectrum during the course of the chemical doping with $NOBF_4$ or the electrochemical doping (at different oxidation potentials) of the α,α′-dimethyl end-capped oligothiophenes[52,53] and in several regioregular polyalkylthiophenes[54,55] (i.e., on going from a heteroaromatic structure of the molecular backbone to a heteroquinonoid one).

The atomic vibrational displacements for the vibrations associated with the most intense Raman bands of Th2CN4 in the 1600−1000 cm^{-1} are sketched in Figure 9. The peaks calculated at 1536 (exp. 1536) and 1502 (exp. 1510) cm^{-1} can be assigned to a stretching vibration of the inter-ring double bond, $\nu(C_\alpha{=}C_\alpha)$, and to the symmetric stretching $\nu_s(C_\beta{=}C_\beta)$ mode, respectively. In both cases, there is an extensive mixing with a symmetric stretching of the $C_\alpha{=}C_{sp2}$ bonds.

The strongest band measured near 1468 cm^{-1} is calculated, after uniform scaling, with a remarkable accuracy at 1466 cm^{-1}. The corresponding normal mode should be described as a totally symmetric ν(CC) vibration, spreading over the whole oligothienoquinonoid spine, in which all double C═C bonds lengthen in-phase while all single C−C bonds shrink in-phase. The stretching of the CC bonds is necessarily coupled with the in-plane bending of the C−H bonds in which the H atoms recoil with a large displacement which opposes that of the C atoms. This normal mode describes the geometrical evolution from the heteroquinonoid to the heteroaromatic configurations of the nuclei, being clearly related to the vibrational coordinate labeled as *Я* in the ECC theory.[45−48]

The modes calculated at 1328 and 1229 (exp. 1346 and 1255) cm^{-1} arise from an antisymmetric and a symmetric stretching of the $C_\alpha{-}C_\beta$ ring bonds, respectively, for which the vibrational

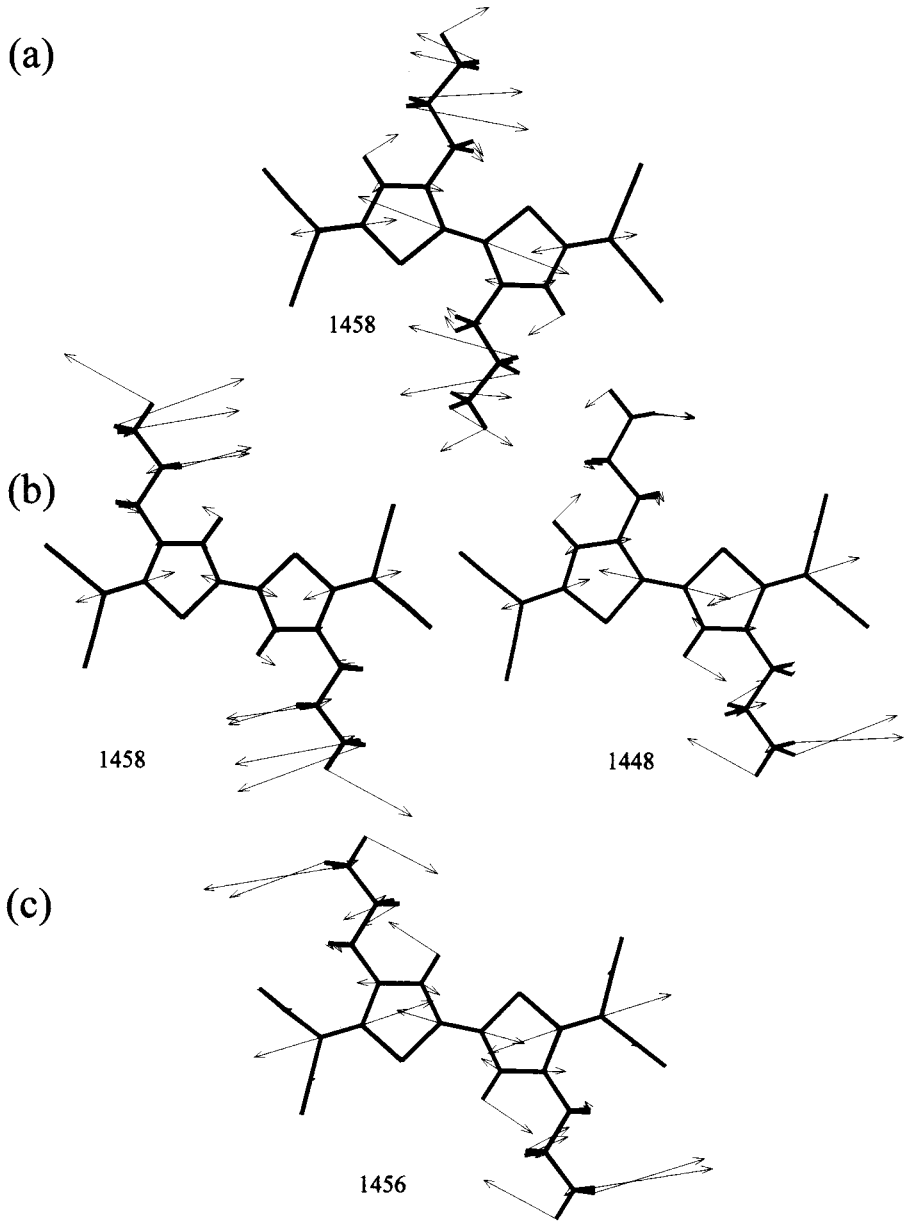

Figure 10. Schematic eigenvectors for the most intense Raman lines at around 1470−1450 cm^{-1} of the HH (a), HT (b), and TT (c) isomers, computed at the B3LYP/6-31G** level.

motions of both thiophene units take place in-phase. The last vibration is coupled to a large extent with the stretching of the C_{sp2}−CN bonds of the dicyanomethylene groups. The peaks measured at 1209 and 1138 cm^{-1} can be correlated with the theoretical modes at 1184 and 1118 cm^{-1}, respectively. Both vibrations are essentially due to stretchings of the single C_α−C_β bonds, slightly mixed with the stretchings of the C_{sp2}−CN bonds. Finally, the band calculated at 1070 (exp. 1092) cm^{-1} is due to the totally symmetric in-plane bendings of the C−H bonds.

Let us focus our attention to the strongest Raman scattering, for which the electron−phonon interaction is the largest. The position of this band is dependent on the molecular size for a given series of oligomers; it shows a continuous redshift as the chain length grows longer. For the *heteroaromatic* series of the α,α′-dimethyl end-capped oligothiophenes in the neutral state,[43,51] the band shifts from 1492 cm^{-1} in the dimer up to 1477 cm^{-1} in the hexamer. This normal mode undergoes a large redshift (appearing near 1415 cm^{-1}) for the radical cations and dications of these materials.[25] The frequency of the strongest Raman band of Th2CN4 is 24 cm^{-1} lower than in the α,α′-dimethyl end-capped bithiophene,[51] and even lower by 9 cm^{-1} than in the corresponding sexithiophene.[43] Thus, we can conclude that the quinoidization of the molecular backbone causes an interaction between the π-electrons systems of the two constituent thienyl moieties much more effective as the increasing number of units in the chain do for the corresponding series of heteroaromatic compounds. The large redshift of the *Я* mode in going to the ionized species is due to the fact that removing electrons from the π-conjugated molecule (an electron-deficient system) softens the bondings of its skeleton, which then can vibrate more easily.

The position of the *Я* mode is also dependent on the substitution pattern of the π-conjugated system, likely due to mass effects on the kinetic G matrix.[38] This is clearly observable in the spectra of the three isomers plotted in Figure 8. The strongest band is measured at 1452 cm^{-1} in the HH, at 1470 cm^{-1} in the TT, and at 1466 or 1452 cm^{-1} in the HT isomer. In general, we have observed that when bulky side groups are attached to the outermost α and/or β positions of the molecule, the line due to the *Я* mode experiences an upshift in frequency.[56]

These dynamical effects could explain the different positions of the strongest Raman band in the HH and TT isomers. The theoretical eigenvectors (sketched in Figure 10) give further support to the assignment of these bands as the Я mode.

V. Conclusions

In this work, we have performed a combined theoretical and experimental study of the effects of the β-alkylation on the electronic and vibrational properties of a bithienoquinonoid compound, in its neutral form. Three different regioregular β,β'-dihexyl substitution patterns were analyzed. The materials possess a highly extended π-electron conjugation and a large nonlinear hyperpolarizability, since they bear a pure heteroquinonoid structure in their electronic ground states. In addition, the coexistence of an electron-rich moiety (the bithiophene spine) and electron-deficient moieties (the dicyanomethylene groups on either side of the molecule) is expected to cause *intramolecular charge transfer*.

Theoretical calculations, at the B3LYP/6-31G** level, indicate that alkyl substitution causes rather small changes in the thiophene ring geometry, and only the equilibrium atomic charges show a significant variation along the series of compounds. In particular, the natural bond orbital atomic charge on the C_β atom attached to the alkyl side chain largely builds up with respect to the unsubstituted molecular backbone. This induces a partial polarization of the double C_β═C_β bonds upon alkylation.

The topological analysis of the charge electronic density, performed within the framework on the atoms-in-molecules theory, shows that two unexpected ring structures appear as a consequence of the closed-shell interactions between the alkyl chain and (i) the S atoms upon substitution in the 3-position, and (ii) the CN groups upon substitution in the 4-position. These ring structures could be the origin for the similar trends showed by the properties related to the charge density of the central double bonds and its neighbors, on one hand, and the outermost double bonds and its neighbors, on the other hand.

The FT-IR and FT-Raman spectra of the compounds were studied in relation to the effective conjugation length in the neutral state. The observation, both in the Raman and the infrared spectra, of a very small number of bands with extralarge intensities is a proof of the existence in this type of system of a strong electron−phonon interaction. The frequency of the ν(C≡N) stretching vibration, measured at around 2215 cm^{-1} in the infrared spectra of the four compounds, lets us estimate a degree of intramolecular charge transfer of about 0.28.

The Raman spectrum of the Th2CN4 *bithienoquinonoid* molecule has been found to be halfway between those of the *heteroaromatic* oligothiophenes in the neutral state and those of their corresponding oxidized species. Thus, the electronic structure of these bithienoquinonoids (which are composed by a positively charged bithiophene spine and two end-caps charged negatively) most likely represents the conjugational defects created upon oxidative doping in polythiophene and the oligothiophenes.

Finally, we have proposed an assignment of the main vibrational bands on the basis of the B3LYP/6-31G** calculations. The DFT eigenvectors for some of the vibrations appearing in the C═C stretching region have enabled us to identify, within the theoretical formalism of the effective conjugation coordinate theory, a few particular normal modes largely involved in π-electron conjugation.

Acknowledgment. The present work was supported by the Dirección General de Enseñanza Superior (DGES, MEC, Spain) through the research Project PB96-0682. We are also indebted to Junta de Andalucía (Spain) funding for our research group (no. FQM-0159). The authors acknowledge the use of the scientific instrumentation and the technical facilities of the Servicio Central de Apoyo a la Investigación (SCAI) of the University of Malaga. J.C. is grateful to the MEC for a personal grant.

Supporting Information Available: Table 1S gives the natural bond orbital atomic charges as derived from the B3LYP/6−31** calculations. Meanwhile, Table 2S gives the topological properties of the electronic charge density, $\rho(\mathbf{r})$, at the bond critical points for the some bonds of the systems under study. Finally, the figure shows the FT-IR spectra of Th2CN4 (a) and of the HH (b), HT (c), and TT (d) regioregular isomers in the 3500−2000 cm^{-1} spectral range. This material is available free of charge via the Internet at http://pubs.acs.org.

References and Notes

(1) Skotheim, T. A. *Handbook of Conducting Polymers*; Marcel Dekker: New York, 1986; Vols. I and II.

(2) Nalwa, H. S. *Handbook of Organic Conductive Molecules and Polymers*; Wiley: Chichester, 1997; Vols. 1−4.

(3) Müllen, K.; Wegner, G. *Electronic Materials: The Oligomer Approach*; Wiley-VCH: Weinheim, 1998.

(4) Tourillon, G.; Garnier, F. *J. Electroanal. Chem. Interfacial Electrochem.* **1982**, *135*, 173.

(5) Hotta, S.; Hosaka, T.; Shimotsuma, W. *Synth. Met.* **1983**, *6*, 69.

(6) Tourillon, G.; Garnier, F. *J. Electrochem. Soc.* **1983**, *130*, 2042.

(7) Heeger, A. J.; Kivelson, S.; Schrieffer, J. R.; Su, W. P. *Rev. Mod. Phys.* **1988**, *60*, 781.

(8) Lu, Y. *Solitons and Polarons in Conducting Polymers*; World Scientific: Singapore, 1983.

(9) Brédas, J. L.; Street, G. B. *Acc. Chem. Res*. **1985**, *18*, 309.

(10) Wada, T.; Wang, L.; Fichou, D.; Higuchi, H.; Ojima, J.; Sasabe, H. *Mol. Cryst. Liq. Cryst.* **1994**, *B255*, 149.

(11) Higuchi, H.; Nakayama, T.; Koyama, H.; Ojima, J.; Wada, T.; Sasabe, H. *Bull. Chem. Soc. Jpn.* **1995**, *68*, 2363.

(12) For example, see Craenen, H. A. H.; Verhoeven, J. W.; de Boer, Th. J. *Tetrahedron Lett.* **1970**, 1167.

(13) Mulliken, R. S. *J. Am. Chem. Soc.* **1952**, *74*, 811.

(14) Higuchi, H.; Yoshida, S.; Uraki, Y.; Ojima, J. *Bull. Chem. Soc. Jpn.* **1998**, *71*, 2229.

(15) Hernandez, V.; Casado, J.; Hotta, S.; Lopez Navarrete, J. T. *Synth. Met.*, in press.

(16) Parr, R. G.; Yang, W. *Density Functional Theory of Atoms and Molecules*; Oxford University Press: New York, 1989.

(17) Labanowski, J. K.; Andzelm, J. W. *Density Functional Methods in Chemistry*; Springer: New York, 1991.

(18) Stephens, P. J.; Devlin, F. J.; Chabalowski, C. F.; Frisch, M. J. *J. Phys. Chem.* **1994**, *98*, 11623.

(19) Scott, A. P.; Radom, L. *J. Phys. Chem.* **1996**, *100*, 16502.

(20) Frisch, M. J.; Trucks, G. W.; Schlegel, H. B.; Gill, P. M. W.; Johnson, B. G.; Robb, M. A.; Cheeseman, J. R.; Keith, T.; Petersson, G. A.; Montgomery, J. A.; Raghavachari, K.; Al-Laham, M. A.; Zakrzewski, V. G.; Ortiz, J. V.; Foresman, J. B.; Cioslowski, J.; Stefanov, B. B.; Manayakkara, A.; Challacombe, M.; Peng, C. Y.; Ayala, P. Y.; Chen, W.; Wong, M. W.; Andres, J. L.; Replogle, E. S.; Gomperts, R.; Martin, R. L.; Fox, D. J.; Binkley, J. S.; Defrees, D. J.; Baker, J.; Stewart, J. P.; Head-Gordon, M.; Gonzalez, C.; Pople, J. A. *Gaussian 94*, revision C.3; Gaussian, Inc.: Pittsburgh, PA, 1995.

(21) Becke, A. D. *J. Chem. Phys.* **1993**, *98*, 5648.

(22) Novoa, J. J.; Sosa, C. *J. Phys. Chem.* **1995**, *99*, 15837.

(23) Rauhut, G.; Pulay, P. *J. Phys. Chem.* **1995**, *99*, 3093.

(24) Francl, M. M.; Pietro, W. J.; Hehre, W. J.; Binkley, J. S.; Gordon, M. S.; Defrees, D. J.; Pople, J. A. *J. Chem. Phys.* **1982**, *77*, 3654.

(25) Casado, J.; Hernandez, V.; Hotta, S.; Lopez Navarrete, J. T. *J. Chem. Phys.* **1998**, *109*, 10419.

(26) Bader, R. F. W. *Atoms in Molecules. A Quantum Theory*; Clarendon Press: Oxford, 1990.

(27) Popelier, P. L. A. *Comput. Phys. Commun.* **1996**, *93*, 212.

(28) Biegler-König, F. W.; Bader, R. F. W.; Wang, T. H. *J. Comput. Chem.* **1982**, *3*, 317.

(29) Reed, A. E.; Weinstock, R. B.; Weinhold, F. *J. Chem. Phys.* **1985**, *83*, 735. Reed, A. E.; Curtiss, L. A.; Weinhold, F. *Chem. Rev.* **1988**, *88*, 899.

(30) Biarge, J. F.; Herranz, J.; Morcillo, J. *Ann. Fis. Quim.* **1961**, *A57*, 81. Person, W. B.; Zerbi, G. *Vibrational Intensities in Infrared and Raman Spectroscopy*; Elsevier: Amsterdam, 1982; Chapter 5.

(31) Eliashevich, M.; Volkenstein, M. *Zh. Eksp. Teor. Fiz.* **1945**, *9*, 101. Gribov, L. A. *Intensity Theory for Infrared Spectra of Polyatomic Molecules*; Consultants Bureau: New York, 1964.

(32) VanStraten, A. J.; Smit, W. A. *J. Mol. Spectrosc.* **1976**, *62*, 297.

(33) Porzio, W.; Destri, S.; Mascherpa, M.; Brückner, S. *Acta Polym.* **1993**, *44*, 266.

(34) Hotta, S.; Waragai, K. *J. Mater. Chem.* **1991**, *1*, 835.

(35) Albrecht, C. A. *J. Chem. Phys.* **1961**, *34*, 1476.

(36) Chappell, J. S.; Bloch, A. N.; Bryden, W. A.; Maxfield, M.; Poehler, T. O.; Cowan, D. O. *J. Am. Chem. Soc.* **1981**, *103*, 2442.

(37) Hernandez, V.; Hotta, S.; Lopez Navarrete, J. T. *J. Chem. Phys.* **1998**, *109*, 2543.

(38) Wilson, E. B. Jr.; Decius, J. C.; Cross, P. C. *Molecular Vibrations*; McGraw-Hill: New York, 1955.

(39) Lopez Navarrete, J. T.; Zerbi, G. *J. Chem. Phys.* **1991**, *94*, 957, 965.

(40) Hernandez, V.; Ramirez, F. J.; Zotti, G.; Lopez Navarrete, J. T. *J. Chem. Phys.* **1993**, *98*, 769.

(41) Hernandez, V.; Ramirez, F. J.; Otero, T. F.; Lopez Navarrete, J. T. *J. Chem. Phys.* **1994**, *100*, 114.

(42) Hernandez, V.; Veronelli, M.; Favaretto, L.; Lopez Navarrete, J. T.; Jones, D.; Zerbi, G. *Acta Pymerica.* **1996**, *47*, 62.

(43) Hernandez, V.; Casado, J.; Ramirez, F. J.; Zotti, G.; Hotta, S.; Lopez Navarrete, J. T. *J. Chem. Phys.* **1996**, *104*, 9271.

(44) Horovitz, B. *Solid State Commun.* **1982**, *41*, 729.

(45) Castiglioni, C.; Gussoni, M.; Lopez Navarrete, J. T.; Zerbi, G. *Solid State Commun.* **1988**, *65*, 625.

(46) Zerbi, G.; Castiglioni, C.; Lopez Navarrete, J. T.; Tian, B.; Gussoni, M.; Zerbi, G. *Synth. Met.* **1989**, *28*, D359.

(47) Castiglioni, C.; del Zoppo, M.; Zerbi, G. *J. Raman Spectrosc.* **1993**, *24*, 485.

(48) Hernandez, V.; Castiglioni, C.; Del Zoppo, M.; Zerbi, G. *Phys. Rev. B.* **1994**, *50*, 9815.

(49) Degli Esposti, A.; Moze, O.; Taliani, C.; Tomkinson, J. T.; Zamboni, R.; Zerbetto, F. *J. Chem. Phys.* **1996**, *104*, 9704.

(50) Ehrendorfer, Ch.; Karpfen, A. *J. Phys. Chem.* **1995**, *99*, 5341.

(51) Hernandez, V.; Casado, J.; Ramirez, F. J.; Zotti, G.; Hotta, S.; Lopez Navarrete, J. T. *Synth. Met.* **1996**, *76*, 277.

(52) Casado, J.; Hernandez, V.; Hotta, S.; Lopez Navarrete, J. T. *Adv. Mater.* **1998**, *10*, 1458.

(53) Casado, J.; Otero, T. F.; Hotta, S.; Hernandez, V.; Ramirez, F. J.; Lopez Navarrete, J. T. *Opt. Mater.* **1998**, *9*, 82.

(54) Pron, A.; Louarn, G.; Laplowski, M.; Zagorska, M.; Glowczyk-zubek, J.; Lefrant, S. *Macromolecules* **1995**, *28*, 4644.

(55) Louarn, G.; Trznadel, M.; Buisson, J. P.; Laska, J.; Pron, A.; Laplowski, M.; Lefrant, S. *J. Phys. Chem.* **1996**, *100*, 12532.

(56) Agosti, E.; Rivola, M.; Hernandez, V.; Del Zoppo, M.; Zerbi, G. *Synth. Met.* **1999**, *100*, 101.